
Target-Aligned Reinforcement Learning

Leonard S. Pleiss
Technical University of Munich
leonard.pleiss@tum.de

James Harrison
Google DeepMind
jamesharrison@google.com

Maximilian Schiffer
Technical University of Munich
schiffer@tum.de

Abstract

Many value-based deep reinforcement learning algorithms rely on target networks—lagged copies of the online network—to stabilize training. While effective, this mechanism introduces a fundamental stability-recency tradeoff: slower target updates improve stability but reduce the recency of learning signals, hindering convergence speed. We propose Target-Aligned Reinforcement Learning (TARL), a simple drop-in refinement for existing algorithms that emphasizes transitions for which the target and online network estimates are highly aligned. By focusing updates on well-aligned targets, TARL mitigates the adverse effects of stale target estimates while retaining the stabilizing benefits of target networks. We empirically demonstrate consistent improvements within discrete and continuous control algorithms across various benchmark environments without any hyperparameter tuning, including a 38.18% peak score gain on Atari-10, while incurring less than a 4% increase in wall-clock time.

1 Introduction

In Reinforcement Learning (RL), agents optimize their policy through repeated interaction with an environment, aiming to maximize expected cumulative return. A central mechanism enabling this process is Temporal Difference (TD) learning [Sutton, 1988], which relies on bootstrapped target estimates—so-called target values. Current state estimates are iteratively updated toward the estimates of future states, thereby allowing the agent to anticipate long-term reward.

However, as shown by Mnih et al. [2015], naïvely using the online network to produce target values can destabilize learning. To address this issue, they introduced a designated target network. A target network is a lagged copy of the online network used exclusively to generate target values. By decoupling the online parameter updates from target value computation, the bootstrapped targets are generated by a comparatively stationary function approximator. This reduces temporal correlations between updates and targets, suppresses self-reinforcing error feedback, and substantially improves training stability and convergence behavior. This innovation contributed to landmark achievements such as human-level performance on the Atari-57 benchmark [Mnih et al., 2015], and target networks remain a cornerstone of many state-of-the-art RL algorithms [Fujimoto et al., 2018, Hessel et al., 2017, Haarnoja et al., 2018, Badia et al., 2020, Schwarzer et al., 2023].

Despite their widespread success, target networks introduce a critical limitation: by construction, their estimates are lagged relative to the online network. The lag can cause target estimates to become stale, reflecting outdated value predictions that no longer align with the current policy or representation [Vincent et al., 2025]. In essence, it creates a dynamic analogous to aiming at a moving target using delayed coordinates: if the value function changes direction, the lagged target steers the update astray.

Consequently, improved target stability necessarily comes at the cost of reduced recency, while increasing recency risks reintroducing instability. This phenomenon constitutes the fundamental *stability-recency tradeoff*: Ideally, target values should be as up-to-date as possible while preserving the level of stability required for reliable bootstrapped learning.

In this work, we argue that sacrificing recency is not necessary to ensure stability. We propose to mitigate this tradeoff by using the unstable but recent online network to validate the stable but partially stale target network. Our approach—Target-Aligned Reinforcement Learning (TARL)—prioritizes updates where online and target estimates agree, enabling the agent to exploit recent information without compromising stability.

Background. Even though individual papers have recently claimed to bypass the need for a target network by proposing alternate update rules [Kim et al., 2019], functional regularization [Piché et al., 2023], decision transformers [Chen et al., 2021] or streaming algorithms [Elsayed et al., 2024], target networks remain the de facto standard in value-based RL. They are a core component in most popular RL algorithms, including Deep Q-Network (DQN), Rainbow, Soft Actor-Critic (SAC) or Deep Deterministic Policy Gradient [Lillicrap et al., 2015, Hessel et al., 2017, Mnih et al., 2015, Haarnoja et al., 2018]. Target networks further remain a cornerstone of state-of-the-art RL algorithms to this day [Badia et al., 2020, Hessel et al., 2017, Haarnoja et al., 2018, Schwarzer et al., 2023].

As such, the stability-recency tradeoff remains a fundamental consideration in RL, particularly during hyperparameter tuning. Most algorithms navigate the tradeoff through design choices that govern the target network’s update mechanism and cadence. There are two major update mechanisms, *hard* and *soft* target network updates [Li, 2023].

Methods like DQN [Mnih et al., 2015] traditionally perform *hard* updates. In some fixed frequency—denoted as the target update interval K —the target network is overwritten by the online network. This frequency is then tuned to balance stability and recency.

Other algorithms like SAC or Deep Deterministic Policy Gradient usually perform *soft* updates [Lillicrap et al., 2015, Kobayashi and Ilboudo, 2021, Haarnoja et al., 2018, Zhang et al., 2021]. A soft update is a mechanism to incrementally adjust the target network’s parameters toward those of the online network. Rather than copying parameters at fixed intervals, the target network is gradually updated at every step. These gradual updates are usually performed via exponential moving or Polyak averages [Polyak and Juditsky, 1992], typically of the form

$$\theta_{\text{target}} \leftarrow \tau \theta_{\text{online}} + (1 - \tau) \theta_{\text{target}}, \tag{1}$$

where $\tau \in (0, 1]$ controls the update magnitude. Soft updates reduce the variance and non-stationarity of bootstrapped targets by smoothing parameter changes over time, improving training stability while still allowing target estimates to track the evolving online network.

Regardless of whether frequent soft updates or infrequent hard updates are employed, the challenge remains the same: to identify an optimal balance where stability is maintained while recency is maximized. Current methods therefore essentially treat this tradeoff as a zero-sum game, merely adjusting the slider between stability (low τ or high K) and recency (high τ or low K).

In contrast, we approach this challenge from a novel angle. We posit that we do not need to make the target network fresher (and more unstable) to improve learning; we only need to filter out updates where the target network’s staleness leads to incorrect update directions. We thus focus on the alignment between the stable estimate—the target network—and the most recent estimate—the online network—on a per-transition basis. We propose to prioritize updates where both target estimates are well-aligned, indicating that our learning target is both stable *and* recent. This perspective bypasses the conventional tradeoff, as it preserves stability without sacrificing recency.

Contribution. Our contribution is threefold: First, we introduce a novel offline-online target alignment metric that quantifies agreement between the online and target network value estimates. Second, we present TARL, an algorithmic framework that integrates target alignment through oversampling into any standard RL algorithm employing target networks. Finally, we support our claims with empirical studies across various discrete and continuous control benchmarks and multiple algorithms, showing that TARL consistently improves performance.

2 Problem statement

We consider a standard Markov decision process (MDP) as usually studied in an RL setting [Sutton and Barto, 2018]. We characterize this MDP as a tuple $(\mathcal{S}, \mathcal{A}, P, r, \gamma, p)$, where \mathcal{S} is a state space, \mathcal{A} is an action space, $P : \mathcal{S} \times \mathcal{A} \rightarrow \Delta(\mathcal{S})$ is a stochastic kernel, $r : \mathcal{S} \times \mathcal{A} \rightarrow \mathbb{R}$ is a reward function, $\gamma \in (0, 1)$ is a discount factor, and $p \in \Delta(\mathcal{S})$ denotes a probability mass function describing the distribution of the initial state, $S_1 \sim p$.

We denote by S_t and A_t the random variables representing the state and action at time t , and by $s \in \mathcal{S}$ and $a \in \mathcal{A}$ their respective realizations. At time step t , the system is in state $S_t \in \mathcal{S}$. If an agent takes action $A_t \in \mathcal{A}$, it receives a corresponding reward $r(s, a)$, and the system transitions to the next state $S_{t+1} \sim P(\cdot | s, a)$. We define the random reward at time t as $R_t = r(S_t, A_t)$. The agent selects actions based on a policy $\pi : \mathcal{S} \rightarrow \mathcal{A}$ via $A_t = \pi(S_t)$. Let $\mathbb{P}_p^\pi(\cdot) = \text{Prob}(\cdot | \pi, S_1 \sim p)$ denote the probability of an event when following a policy π , starting from an initial state $S_1 \sim p$, and let $\mathbb{E}_p^\pi[\cdot]$ denote the corresponding expectation operator. Let n denote the number of transitions within the episode. Let G_t denote the discounted return at time t , with

$$G_t = \sum_{i=t}^n \gamma^{i-t} R_i. \quad (2)$$

We define the Q-function (or action-value function) for a policy π as

$$Q_t^\pi(s, a) = \mathbb{E}_p^\pi[G_t | S_t = s, A_t = a] \quad (3)$$

$$= \mathbb{E}_p^\pi \left[\sum_{i=t}^n \gamma^{i-t} R_i | S_t = s, A_t = a \right]. \quad (4)$$

The ultimate goal of value-based RL is to learn a policy that maximizes the Q-function, leading to $Q^*(s, a) = \max_\pi Q^\pi(s, a)$.

The policy is gradually improved by repeatedly interacting with the environment and learning from previously experienced transitions. A transition C_t is a 5-tuple, $C_t = (S_t, A_t, R_t, S_{t+1}, d_t)$, where d_t is a binary episode termination indicator, $d_t = \mathbb{1}_{t=n}$. One popular approach to learn Q^* is via Watkins' Q-learning (Watkins [1989], Watkins and Dayan [1992]), where Q-values are gradually updated via

$$Q(S_t, A_t) \leftarrow Q(S_t, A_t) + \eta \cdot \delta_t, \quad (5)$$

with $\eta \in (0, 1]$ being the learning rate and δ_t being the TD error. In the classical tabular formulation, this TD error is defined using the *online target*,

$$Q_{\text{target}}(S_t) = R_t + (1 - d_t) \cdot \gamma \cdot \max_a Q(S_{t+1}, a, \theta), \quad (6)$$

yielding the online TD error $\delta_t = Q_{\text{target}}(S_t) - Q(S_t, A_t, \theta)$.

In deep RL, and specifically in the DQN algorithm [Mnih et al., 2015], stability is improved by introducing a separate *target network* with parameters $\bar{\theta}$. Crucially, $\bar{\theta}$ is a time-lagged copy of the online parameters θ , such that, under hard updates, $\bar{\theta} \approx \theta_{t-k}$ for some delay k . This target network improves training stability: When a single function approximator is used to both estimate action values and define the bootstrap targets, parameter updates induce correlated changes in predictions and targets, which can lead to divergence. The target network mitigates this issue by decoupling target computation from the online updates, yielding a temporally more stationary learning objective.

The *offline target*—i.e., the target value from the target network, as used in standard DQN—is defined as

$$\bar{Q}_{\text{target}}(S_t) = R_t + (1 - d_t) \cdot \gamma \cdot \max_a Q(S_{t+1}, a, \bar{\theta}), \quad (7)$$

which leads to the offline or target TD error $\bar{\delta}_t = \bar{Q}_{\text{target}}(S_t) - Q(S_t, A_t, \theta)$.

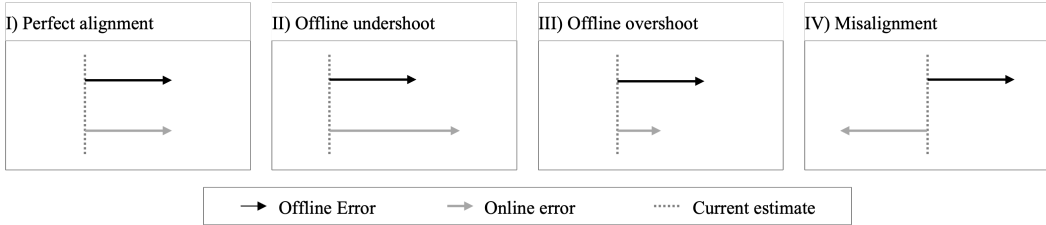


Figure 1: Stylized visualization of alignment scenarios. We distinguish between updates fully supported by the online network (scenario I & II) and updates that are only partially or not at all supported by the online network (scenario III & IV). We posit that update types I and II are safer than update types III and IV.

3 Target-Aligned Reinforcement Learning

In this section, we present TARK, a framework designed to mitigate the stability-recency tradeoff in deep RL. We first build the intuition for target alignment by analyzing the interplay between offline and online value estimates. We then formalize this intuition into a computable alignment score. Finally, we introduce an alignment-based oversampling mechanism that integrates this metric into standard off-policy algorithms to prioritize stable *and* recent updates.

3.1 Target alignment

In contemporary deep RL, value estimates are updated using target values provided by a lagged offline network. While this lag increases stability, it naturally sacrifices recency. TARK resolves this by quantifying the agreement between the stable (offline) target and the most recent (online) estimate. Specifically, it measures the extent to which the update direction and magnitude proposed by the offline target are *supported* by the online network. As displayed in Figure 1, we identify four distinct alignment scenarios.

I) Perfect Alignment. The offline and online updates are identical. The offline target is perfectly aligned with the most recent estimate from the online network.

II) Offline Undershoot. Both networks agree on direction, but the online network proposes a more extreme update. The conservative offline update is therefore *fully supported* by the online view. We treat this as a safe update: the stable target points in the right direction but is simply more cautious than the volatile online network.

III) Offline Overshoot. Both networks agree on direction, but the offline target proposes a more extreme update than the online network. The offline update is therefore only *partially supported*, indicating some level of risk that the frozen offline target overshoots the ideal update magnitude, introducing the potential need for partial update reversion in the future. In essence, the stale target may push the agent too hard, ignoring recent evidence that the value is actually closer than the offline target suggests.

IV) Misalignment. The networks disagree on update direction. The offline target is not at all supported by the current online estimate.

We hypothesize that, all else equal, updates with higher online support are more beneficial for learning. Specifically, we posit that learning is most effective in scenarios I and II, where the recent online target fully supports the stable offline target. Conversely, scenarios III and IV introduce varying degrees of risk. In the following section, we define a metric to formalize the established preference for updates with aligned targets.

3.2 Target alignment score

In the following, we formalize the intuition derived in Section 3.1 into a computable *Target Alignment Score* \mathcal{A}_t . This score quantifies, on a per-transition basis, the degree to which the update step proposed by the stable target network is supported by the most recent online estimate. As such, it provides a principled signal for identifying updates that are both stable and up-to-date.

We first define the residual online error δ_t^{next} , which approximates the online error that would remain after applying the update proposed by the offline target under unit step-size,

$$\delta_t^{\text{next}} = \delta_t - \bar{\delta}_t. \quad (8)$$

Using this residual, we define the base alignment score $\mathcal{A}_t^{base} \in [0, 1]$, which measures the extent to which the offline update reduces the magnitude of the current online error,

$$\mathcal{A}_t^{base} = \frac{|\delta_t|}{|\delta_t| + |\delta_t^{next}| + \epsilon}. \quad (9)$$

The denominator $|\delta_t| + |\delta_t^{next}|$ represents the total variation in error space, and $\epsilon = 10^{-8}$ is a small constant added for numerical stability. We choose this specific fractional formulation over simpler alternatives—such as unbounded dot products or purely directional cosine similarities—because it yields a bounded $[0, 1]$ score that rigorously penalizes magnitude disagreements independent of the absolute scale of the TD errors. If the residual error $|\delta_t^{next}|$ is small relative to the initial error $|\delta_t|$, base alignment is high. In the ideal scenario where the offline update fully resolves the online error (i.e., $\delta_t^{next} \rightarrow 0$), the score is maximized (i.e., $\mathcal{A}_t^{base} \rightarrow 1$). Conversely, in cases of Misalignment (Scenario IV) or severe Offline Overshoot (Scenario III), the proposed update exacerbates the residual error, causing the denominator to grow relative to the numerator and diminishing the score towards zero.

However, strict adherence to this base metric would penalize offline over- and undershoots equally. Yet, as established in Section 3.1, in the case of an Offline Undershoot (Scenario II), the designated target is fully supported by the most recent estimate, while it is only partially supported in the Offline Overshoot case (Scenario III). As such, offline undershoots are inherently safer, whereas offline overshoots pose a risk of inducing parameter oscillation. To account for this asymmetry, we define the final alignment metric \mathcal{A}_t ,

$$\mathcal{A}_t = \begin{cases} 1 & \text{if } (\delta_t \cdot \bar{\delta}_t > 0) \text{ and } (|\delta_t| \geq |\bar{\delta}_t|) \\ \mathcal{A}_t^{base} & \text{else.} \end{cases} \quad (10)$$

This metric formally captures our previous visual intuition: The conditional check isolates updates where the direction is identical and the offline magnitude is conservative. Consequently, the score equals one for Perfect Alignment (Scenario I) and Offline Undershoots (Scenario II), while falling back to the strictly penalizing \mathcal{A}_t^{base} for Offline Overshoots (Scenario III) and Misalignments (Scenario IV).

Note on online target stability. The proposed methodology relies on the alignment between online and offline targets. In the broader literature, online targets are often considered too unstable to yield valuable information. However, this instability arises primarily when the online network is used to provide bootstrapped learning targets, as this creates immediate feedback loops. In TARK, the online network is used only for directional validation. As long as the online network is updated based on stable targets provided by the offline network, its estimates remain sufficiently stable to serve as a directional reference for alignment.

3.3 Alignment-based oversampling

Building on the intuition that well-aligned targets yield more reliable learning signals, we introduce a simple extension to standard RL pipelines that explicitly incorporates target alignment to improve sample efficiency. We propose *alignment-based oversampling*, which serves as the backbone for TARK: Given a target batch size m and an oversampling margin $b \in \mathbb{N}$, we sample $m + b$ transitions from the replay buffer, compute their target alignment \mathcal{A}_t , and select the m transitions with the highest alignment for the network update. This mechanism effectively acts as a dynamic noise filter. By temporarily omitting poorly aligned transitions, it defers their updates until subsequent network parameter changes naturally clarify the alignment signal.

Crucially, this building block is a drop-in refinement that effortlessly converts any off-policy RL algorithm employing target networks into its target-aligned version. Algorithm 1 presents an instantiation for Target-Aligned DQN (TA-DQN). Note the boxed lines, which highlight that TARK requires only a localized, minimal modification to the standard training loop. Alternative approaches to integrating alignment, such as prioritized sampling or loss weighting, are discussed in Appendix A.

3.4 Algorithmic intuition

Our hypothesis that—all else equal—updates with higher online support are more beneficial for learning can be understood through three complementary observations, each pointing to the same underlying principle: disagreement between online and offline estimates signals unreliable targets.

Algorithm 1 Target-Aligned Deep Q-Network (TA-DQN)

Input: Replay buffer \mathcal{D} , discount factor γ , batch size m , oversampling margin b , target update interval K , budget T
Initialize $Q(s, a, \theta)$ with parameters θ ; $Q'(s, a, \bar{\theta})$ with parameters $\bar{\theta} \leftarrow \theta$; $\mathcal{D} \leftarrow \emptyset$
Sample initial state $S_1 \sim p$
for $t = 1, \dots, T$ **do**
 Select action A_t using ϵ -greedy policy w.r.t. $Q(S_t, \cdot, \theta)$
 Execute A_t , observe reward R_t and next state S_{t+1}
 Store transition $C_t = (S_t, A_t, R_t, S_{t+1}, d_t)$ in \mathcal{D}

Sample random oversized minibatch $\{M_j\}_{j=1}^{m+b}$ from \mathcal{D}
Compute offline target $\bar{Q}_{\text{target}}(S_j)$, online target $Q_{\text{target}}(S_j)$ and alignment metric A_j for M_j
Obtain final minibatch $\mathcal{C} \leftarrow \text{TopK}_m(M, \mathcal{A})$

 Update θ by minimizing loss, $L(\theta) = \frac{1}{m} \sum_{j=1}^m (\bar{Q}_{\text{target}}(S_j) - Q(S_j, A_j, \theta))^2$
 if $t \pmod K = 0$ **then**
 Update target network: $\bar{\theta} \leftarrow \theta$
 end if
end for

Avoidance of outdated targets. Misalignment or offline overshoots suggest that the proposed offline update is no longer fully supported by the online estimate. By performing updates on those targets, we effectively chase targets which are no longer aligned with the most recent information. Avoiding such updates prevents the agent from committing to update steps that have been identified as directionally incorrect or excessively large by the most recent value estimates.

Temporal ensembling. The online and offline networks provide complementary estimates of the same value function. While they are correlated, they function as a temporal ensemble. Lower agreement between them may indicate higher epistemic target value uncertainty. Prioritizing alignment then acts as a variance reduction mechanism, filtering updates where the target is noisy.

Reversion of misaligned changes. Since the target network is periodically updated with online parameters, online target values eventually become the new offline target values. Consequently, updates based on the current offline target that are misaligned with the current online view are likely to be reverted once the target network updates. As such, Q-value updates based on misaligned targets induce oscillatory behavior and are potentially wasteful.

Implicit stratification. Unlike traditional prioritization schemes, alignment-based selection naturally counteracts rigid sampling biases within its priority distribution via two primary mechanisms: First, within a target update interval, alignment starts out at 1 and decays as updates shift value estimates. Crucially, we expect this decay to be faster for actively sampled transitions, as they are modulated directly. Consequently, the algorithm organically de-prioritizes recently sampled experiences. Second, alignment prioritization avoids structural bias by regular resets: Under a hard update regime, synchronizing the target network instantly resets the target alignment to 1 across the entire replay buffer. This periodic global reset frequently reintroduces temporarily neglected transitions into the active pool with maximum priority. By routinely clearing the priority landscape, the algorithm destroys localized biases. This principle naturally extends to soft update regimes, where continuous parameter tracking gradually realigns target and online estimates, ensuring that the priority of neglected transitions smoothly recovers over time.

A bias-variance perspective. Our previous observations allow a unified interpretation through the bias-variance lens. TARD's empirical success admits a compact reading: *the per-transition alignment score signals that the bias of the offline target has not yet manifested on a given transition.* Existing target-network schemes navigate this axis *globally* via K or τ , whereas TARD navigates it *per transition*.

We treat each bootstrapped TD residual as a noisy estimate of the expected true residual at the current Bellman fixed point, which is 0; variance is taken over training stochasticity (gradient noise, replay sampling) and bias is measured relative to δ_t^* , not to Q^* . The offline residual $\bar{\delta}_t$ then has *low variance*— $\bar{\theta}$ is held constant or smoothed over many updates—but carries *bias* growing with

its staleness. The online residual δ_t is the converse: continually refreshed, hence low-bias but high-variance. Traditional algorithms must select a static point along this Pareto frontier.

TARL changes neither the estimator’s bias nor variance, and does not replace the offline target in the gradient step. It conditions the update on an event—agreement between δ_t and $\bar{\delta}_t$ —correlated with low effective bias. Decomposing the disagreement,

$$\delta_t - \bar{\delta}_t = \underbrace{(\beta_{\delta_t} - \beta_{\bar{\delta}_t})}_{\text{systematic gap}} + \underbrace{(\nu_{\delta_t} - \nu_{\bar{\delta}_t})}_{\text{stochastic gap}}, \quad (11)$$

with β, ν denoting bias and noise components, the small variance of $\bar{\delta}_t$ implies that small disagreement is, up to online noise, evidence that offline bias has not yet diverged on that transition. The same decomposition recovers the asymmetry of A_t in Eq. (10): Scenario II is the low-bias regime where we accept variance reduction by retaining the conservative offline magnitude; Scenario III flags an offline magnitude likely biased upward by staleness; Scenario IV indicates that the directional component of the bias dominates the stochastic gap entirely.

A caveat is in order. Since $\bar{\theta}$ is a delayed copy of θ , both estimators share a common ancestor and could, in principle, agree by failing in the same direction. However, agreement nonetheless remains a highly informative filter. Since the last target synchronization, the online network has absorbed gradient information from numerous transitions that the offline copy has not seen. While co-failure remains possible in deep non-convex optimization, empirical performance suggests that filtering out *known* disagreements successfully prevents the agent from committing to actively conflicting, oscillatory updates. In practice, target alignment serves as a necessary, if not strictly sufficient, condition for reliable learning steps.

4 Numerical results

We evaluate TARL across both continuous and discrete control domains to assess its generality. Our experimental design is chosen to test the hypothesis that target alignment is a fundamental principle, agnostic to the specific algorithm, target update mechanism, or experience replay mechanism. We test this hypothesis in discrete control environments using DQN with uniform sampling, Prioritized Experience Replay (PER) and Reliability-adjusted Prioritized Experience Replay (ReaPER), as well as in continuous control environments using SAC. This selection allows us to test performance across substantially different learning dynamics, action modalities, target value formulations, experience replay strategies and target network update regimes. Specifically, we evaluate TARL in three distinct experimental settings:

Discrete control: We evaluate the impact of Target Alignment in a Double Deep Q-Network (DDQN) using hard target updates on the ATARI-10 benchmark, which approximates the median score across the seminal ATARI-57 benchmark within one percent of variance [Aitchison et al., 2022].

Continuous control: We further evaluate the impact of Target Alignment in SAC using soft target updates on six continuous control environments [Todorov et al., 2012].

Ablations: To better understand the inner workings of TARL, its sensitivity to the oversampling margin, as well as its compatibility with prioritized replay methods, we conduct additional experiments within four MINATAR environments [Young and Tian, 2019].

Crucially, we performed no hyperparameter tuning for TARL. We applied TARL as a direct drop-in refinement without re-tuning the base hyperparameters of the original algorithms. While we added an ablation on the TARL-specific oversampling hyperparameter b , we did not tune b for the main experiments, but fixed $b = m$. This design choice aims to show the flexibility and robustness of TARL, and highlights its ease of integration into existing pipelines.

Evaluation metric. To evaluate learning efficiency and asymptotic performance simultaneously, our primary evaluation metric is the normalized Area Under Curve (nAUC). This metric yields a unitless score in $[0, 1]$, where 0 indicates performance no better than a random agent throughout training, and 1 represents achieving peak performance immediately, rewarding both sample-efficient convergence and high asymptotic returns. A formal definition is provided in Appendix D.

For additional details on our experimental setting, we refer to Appendix B. For per-game and per-seed curves and nAUC tables for all experiments, we refer to Appendix F and G.

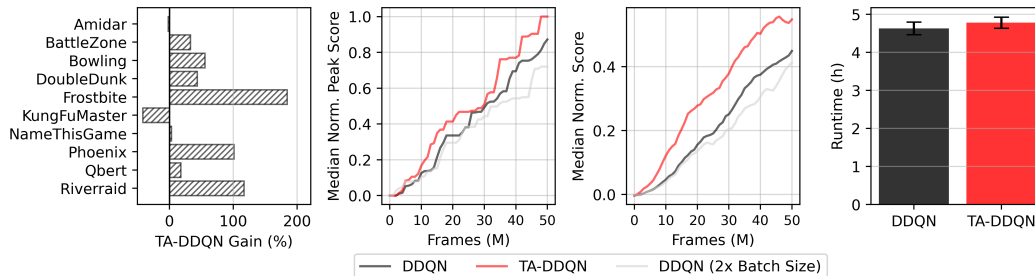


Figure 2: Comparison of DDQN, Target-aligned DDQN (TA-DDQN), and DDQN with doubled batch size across the Atari-10 benchmark. (Left) Per-game peak score improvement of TA-DDQN over DDQN (%). (Center-left) Median normalized cumulative maximum score aggregated over all games as a function of environment frames. (Center-right) Median normalized score over training, reflecting instantaneous rather than best-seen performance. (Right) Mean wall-clock runtime for DDQN and TA-DDQN. Score normalization per game is performed using the range between the random baseline and the best observed performance across all conditions. Score curves are smoothed over 10 evaluations.

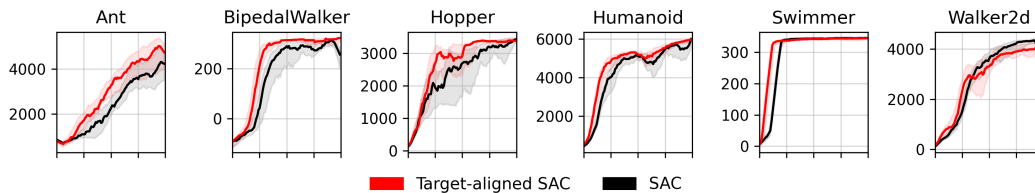


Figure 3: Performance comparison between SAC and target-aligned SAC on six continuous control environments over five seeds. Curves represent median returns, smoothed over 10 evaluations, and shaded areas indicate interquartile ranges.

Discrete control. We compared DDQN performance with and without TARD along the ATARI-10 benchmark. As displayed in Figure 2, Target-Aligned DDQN (TA-DDQN) achieves higher peak scores than its vanilla counterpart in eight out of ten games. TA-DDQN achieved a median peak score gain of 38.18% (95% CI = [3.64, 98.69]; Mean=51.17% (SD=63.03)). Further, TA-DDQN scores a higher nAUC on all games, achieving an average nAUC gain of 151.88% ($SD = 135.76$). Notably, TA-DDQN achieved this outperformance while incurring negligible increases in wall-clock time: TA-DDQN trained for 4.78 hours ($SD=0.15$ hours) on average, vanilla DDQN trained for 4.63 hours ($SD=0.17$ hours). Thus, TARD incurred an overhead in wall-clock time of merely 3.29%.

To control for the confounding effect of additional network evaluations, we evaluated a vanilla DDQN using a doubled batch size. This baseline performs the same number of forward passes as TA-DDQN, but applies backward passes to twice as many transitions. This variant is outperformed by both TA-DDQN and DDQN.

Continuous control. We compared SAC performance with and without TARD along six different continuous control environments, namely ANT, BIPEDALWALKER, HOPPER, HUMANOID, SWIMMER, and WALKER2D. As in Haarnoja et al. [2018], we report performances across five seeds. As displayed in Figure 3, Target-Aligned SAC (TA-SAC) achieved faster convergence than SAC in five out of six environments, slightly underperforming in WALKER2D (-0.7 nAUC). Nonetheless, across all environments, TA-SAC achieves a robust nAUC gain of 10.65% ($SD = 7.46$). Unlike DDQN, where additional online forward passes can be effectively amortized via parallelization, vanilla SAC does not perform online forward passes on sampled batches. Consequently, the naïve implementation of TA-SAC introduces a 17.82% ($SD = 3.44$) increase in wall-clock training time. Yet, the performance gains in this regime highlight that even within modern algorithms under soft updates, explicit alignment filtering improves training dynamics.

Ablation 1: Experience replay. We compared DQN performance with and without TARD for three different experience replay strategies, namely uniform sampling, PER [Schaul et al., 2015] and ReaPER [Pleiss et al., 2025]. We record performance across five seeds [Haarnoja et al., 2018]. Target-aligned methods consistently outperform their non-aligned counterpart, as shown in Figure 4, indicating that TARD is orthogonal to the replay strategy. The outperformance is extremely robust:

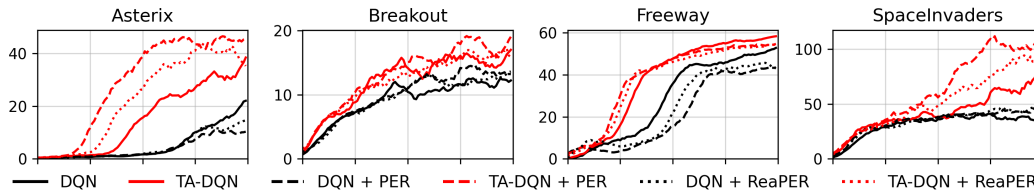


Figure 4: Performance comparison between DQN and target-aligned DQN under different experience replay strategies on four games of the MINATAR benchmark over five seeds. Curves represent median returns, smoothed over 10 evaluations.

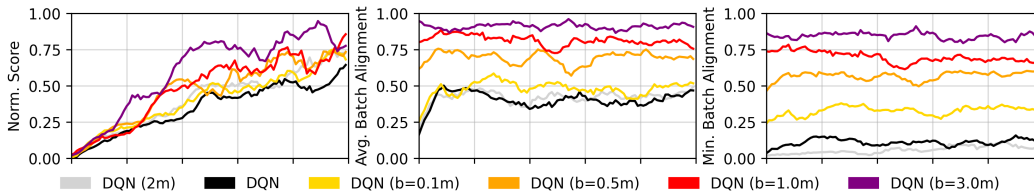


Figure 5: Impact of the oversampling margin on performance and batch alignment. Results are aggregated across four MinAtar environments. The subplots compare standard DQN and a DQN with doubled batch size—denoted as DQN (2m)—against TA-DQN, evaluated at oversampling margins ($b \in \{0.1m, 0.5m, 1.0m, 3.0m\}$). All curves are smoothed over 10 evaluations. (Left) Median normalized evaluation scores. Scores were min-max normalized per environment prior to aggregation. (Center) Average batch alignment post-discard. (Right) Minimum batch alignment post-discard.

It does not only show on average across seeds, but also in every single seed individually (see Figure 9-11).

Ablation 2: Oversampling margin. We further conducted an ablation to evaluate the impact of oversampling margin (Figure 5). We report the normalized scores across the environments, as well as the minimum and mean batch alignment score. Our findings suggest that performance generally increases with growing oversampling margin. Naturally, minimum and mean batch alignment increase as well, and are close to saturation at around 0.9 when $b = 3m$.

5 Discussion

Across a diverse set of environments, for multiple algorithms, and under both hard and soft target network update regimes, algorithms employing TARD consistently outperform their counterparts without alignment correction. Importantly, these improvements are achieved without any additional hyperparameter tuning, highlighting the robustness of the proposed approach. Moreover, TARD can be seamlessly integrated into existing RL pipelines, making it a practical drop-in enhancement that consistently improves performance across multiple domains.

While TARD improves performance, it naturally introduces computational overhead by increasing the number of forward passes required during training. However, because forward passes are relatively inexpensive and highly parallelizable in modern RL frameworks, the impact on wall-clock time remains modest given sufficient device memory, particularly in algorithms natively employing online batch forward passes like DDQN (incurring a mere 3.29% increase for $b = m$ in Atari). Thus, to optimally balance computational costs with performance benefits, the oversampling margin b should simply be scaled to device limits: Figure 5 indicates that larger values of b yield strictly stronger gains. Consequently, we recommend setting b such that the total query size $m + b$ matches the maximum single-pass batch size supported by the available hardware.

Conclusion. We introduced TARD, a method that prioritizes updates on transitions with high target alignment between offline and online targets. Central to our approach is a novel alignment metric that quantifies the consistency between update targets across target network updates. By leveraging this metric as a transition selection criterion, TARD promotes target recency *and* stability, thereby mitigating the stability-recency tradeoff induced by target networks. Empirical evaluation across a variety of benchmarks and algorithms validates TARD’s effectiveness.

TARD can be seamlessly integrated into existing RL pipelines without requiring additional hyperparameter tuning. Beyond its immediate practical benefits, our work highlights a fundamental insight:

the online network—despite being too unstable to provide reliable bootstrap targets—holds highly valuable information for directional update validation. We hope TARL inspires further research into overcoming the structural bottlenecks of value-based RL. Promising future directions include the design of fully differentiable alignment-aware loss functions and the exploration of alignment signals for dynamic representation learning.

References

- Matthew Aitchison, Penny Sweetser, and Marcus Hutter. Atari-5: Distilling the Arcade Learning Environment down to Five Games, 2022. URL <https://arxiv.org/abs/2210.02019>.
- Adrià Puigdomènech Badia, Bilal Piot, Steven Kapturowski, Pablo Sprechmann, Alex Vitvitskyi, Daniel Guo, and Charles Blundell. Agent57: Outperforming the Atari Human Benchmark, 2020. URL <https://arxiv.org/abs/2003.13350>.
- Lili Chen, Kevin Lu, Aravind Rajeswaran, Kimin Lee, Aditya Grover, Michael Laskin, Pieter Abbeel, Aravind Srinivas, and Igor Mordatch. Decision transformer: Reinforcement learning via sequence modeling, 2021. URL <https://arxiv.org/abs/2106.01345>.
- Mohamed Elsayed, Gautham Vasan, and A. Rupam Mahmood. Deep reinforcement learning without experience replay, target networks, or batch updates. In *NeurIPS 2024 Workshop on Fine-Tuning in Modern Machine Learning: Principles and Scalability*, 2024. URL <https://openreview.net/forum?id=yqQJGTDXN>.
- Scott Fujimoto, Herke van Hoof, and David Meger. Addressing function approximation error in actor-critic methods, 2018. URL <https://arxiv.org/abs/1802.09477>.
- Tuomas Haarnoja, Aurick Zhou, Pieter Abbeel, and Sergey Levine. Soft Actor-Critic: Off-Policy Maximum Entropy Deep Reinforcement Learning with a Stochastic Actor, 2018. URL <https://arxiv.org/abs/1801.01290>.
- Matteo Hessel, Joseph Modayil, Hado van Hasselt, Tom Schaul, Georg Ostrovski, Will Dabney, Dan Horgan, Bilal Piot, Mohammad Azar, and David Silver. Rainbow: Combining Improvements in Deep Reinforcement Learning, 2017. URL <https://arxiv.org/abs/1710.02298>.
- Seungchan Kim, Kavosh Asadi, Michael Littman, and George Konidaris. Deepmellow: Removing the need for a target network in deep q-learning. In *Proceedings of the Twenty-Eighth International Joint Conference on Artificial Intelligence, IJCAI-19*, pages 2733–2739. International Joint Conferences on Artificial Intelligence Organization, 7 2019. doi: 10.24963/ijcai.2019/379. URL <https://doi.org/10.24963/ijcai.2019/379>.
- Taisuke Kobayashi and Wendyam Eric Lionel Ilboudo. t-soft update of target network for deep reinforcement learning. *Neural Networks*, 136:63–71, 2021. ISSN 0893-6080. doi: <https://doi.org/10.1016/j.neunet.2020.12.023>. URL <https://www.sciencedirect.com/science/article/pii/S0893608020304482>.
- Shengbo Eben Li. *Deep Reinforcement Learning*, pages 365–402. Springer Nature Singapore, Singapore, 2023. ISBN 978-981-19-7784-8. doi: 10.1007/978-981-19-7784-8_10. URL https://doi.org/10.1007/978-981-19-7784-8_10.
- Timothy P. Lillicrap, Jonathan J. Hunt, Alexander Pritzel, Nicolas Heess, Tom Erez, Yuval Tassa, David Silver, and Daan Wierstra. Continuous control with deep reinforcement learning, 2015. URL <https://arxiv.org/abs/1509.02971>.
- Volodymyr Mnih, Koray Kavukcuoglu, David Silver, Andrei A. Rusu, Joel Veness, Marc G. Belle-mare, Alex Graves, Martin Riedmiller, Andreas K. Fidjeland, Georg Ostrovski, Stig Petersen, Charles Beattie, Amir Sadik, Ioannis Antonoglou, Helen King, Dharshan Kumaran, Daan Wierstra, Shane Legg, and Demis Hassabis. Human-level control through deep reinforcement learning. *Nature*, 518(7540):529–533, February 2015. ISSN 0028-0836, 1476-4687. doi: 10.1038/nature14236. URL <https://www.nature.com/articles/nature14236>.
- Alexandre Piché, Valentin Thomas, Rafael Pardini, Joseph Marino, Gian Maria Marconi, Christopher Pal, and Mohammad Emtiyaz Khan. Bridging the gap between target networks and functional regularization, 2023. URL <https://arxiv.org/abs/2106.02613>.
- Leonard S. Pleiss, Tobias Sutter, and Maximilian Schiffer. Reliability-adjusted prioritized experience replay, 2025. URL <https://arxiv.org/abs/2506.18482>.

- B. T. Polyak and A. B. Juditsky. Acceleration of stochastic approximation by averaging. *SIAM Journal on Control and Optimization*, 30(4):838–855, 1992. doi: 10.1137/0330046. URL <https://doi.org/10.1137/0330046>.
- Antonin Raffin. RL baselines3 zoo. <https://github.com/DLR-RM/rl-baselines3-zoo>, 2020.
- Tom Schaul, John Quan, Ioannis Antonoglou, and David Silver. Prioritized Experience Replay. 2015. doi: 10.48550/ARXIV.1511.05952. URL <https://arxiv.org/abs/1511.05952>.
- Max Schwarzer, Johan Obando-Ceron, Aaron Courville, Marc Bellemare, Rishabh Agarwal, and Pablo Samuel Castro. Bigger, Better, Faster: Human-level Atari with human-level efficiency, 2023. URL <https://arxiv.org/abs/2305.19452>.
- Richard Sutton. Learning to predict by the method of temporal differences. *Machine Learning*, 3: 9–44, 08 1988. doi: 10.1007/BF00115009.
- Richard S. Sutton and Andrew G. Barto. *Reinforcement Learning: An Introduction*. The MIT Press, second edition, 2018. URL <http://incompleteideas.net/book/the-book-2nd.html>.
- Emanuel Todorov, Tom Erez, and Yuval Tassa. Mujoco: A physics engine for model-based control. In *2012 IEEE/RSJ International Conference on Intelligent Robots and Systems*, pages 5026–5033, 2012. doi: 10.1109/IROS.2012.6386109.
- Hado van Hasselt, Arthur Guez, and David Silver. Deep reinforcement learning with double q-learning, 2015. URL <https://arxiv.org/abs/1509.06461>.
- Théo Vincent, Yogesh Tripathi, Tim Faust, Yaniv Oren, Jan Peters, and Carlo D’Eramo. Bridging the performance gap between target-free and target-based reinforcement learning, 2025. URL <https://arxiv.org/abs/2506.04398>.
- Christopher Watkins. *Learning From Delayed Rewards*. PhD thesis, Kings College, London, 1989.
- Christopher J. C. H. Watkins and Peter Dayan. Q-learning. *Machine Learning*, 8(3-4):279–292, May 1992. ISSN 0885-6125, 1573-0565. doi: 10.1007/BF00992698. URL <http://link.springer.com/10.1007/BF00992698>.
- Kenny Young and Tian Tian. Minatar: An atari-inspired testbed for thorough and reproducible reinforcement learning experiments, 2019. URL <https://arxiv.org/abs/1903.03176>.
- Hongming Zhang, Fengshuo Bai, Chenjun Xiao, Chao Gao, Bo Xu, and Martin Müller. Beta-dqn: Improving deep q-learning by evolving the behavior, 2025.
- Shangdong Zhang, Hengshuai Yao, and Shimon Whiteson. Breaking the deadly triad with a target network. In Marina Meila and Tong Zhang, editors, *Proceedings of the 38th International Conference on Machine Learning*, volume 139 of *Proceedings of Machine Learning Research*, pages 12621–12631. PMLR, 18–24 Jul 2021. URL <https://proceedings.mlr.press/v139/zhang21y.html>.

A Alternative integration strategies

Several alternatives to oversampling are worth considering to integrate alignment into the learning process:

Prioritized sampling. Replay transitions could be sampled based on alignment, favoring well-aligned updates. However, this would require computing alignment for the full buffer, which is computationally prohibitive. Approximate solutions, such as maintaining stored alignment values updated on sampling (analogous to Prioritized Experience Replay [Schaul et al., 2015]), are likely not applicable, as the alignment metric relies on frequently changing online estimates.

Loss weighting. Alignment can be used as a weight within the loss function, upweighting well-aligned samples and downweighting poorly aligned ones. While flexible, this approach requires hyperparameter tuning and may interfere with other loss-weighting schemes (e.g., importance sampling in PER), thereby limiting the method’s general applicability.

Loss scaling. Alternatively, alignment may be used to directly scale the loss, effectively modulating the learning rate on a per-sample basis. This is conceptually clean but risks destabilization unless normalization or re-scaling strategies are applied, requiring careful hyperparameter tuning.

We consider oversampling the most robust and conceptually sound approach, as it does not require hyperparameter tuning, is easily integrated into existing pipelines and ensures target alignment while causing limited computational overhead. We therefore deliberately chose to limit this paper’s scope to oversampling. Yet, we plan to pursue other directions in future work.

B Experimental design

Hyperparameters for SAC were set to the standards defined in the RL Baselines3 Zoo [Raffin, 2020]. In ANT, BIPEDALWALKER, HOPPER, SWIMMER, and WALKER2D, we trained for 1 million timesteps per run. In HUMANOID, we trained for 2 million timesteps per run. DQN hyperparameters for MINATAR were set to recommendations published within Zhang et al. [2025]. We trained for 2 million timesteps per run. DDQN hyperparameters for ATARI were set in accordance with seminal work [Mnih et al., 2015, Schaul et al., 2015, van Hasselt et al., 2015]. We trained for 50 million frames (12.5 million timesteps) per run. PER and ReaPER were configured as in the original work [Schaul et al., 2015, Pleiss et al., 2025]. Importance sampling weights are batch-normalized by division with the maximum weight within the (filtered) batch. When using TARL with PER or ReaPER, sampling priorities are updated for the enlarged batch. Oversampling margins are, when required, converted to integers via flooring (i.e., when $b = 32$ and $b = 0.1m$, $b \leftarrow 3$). Atari experiments employ the standard modification steps extensively described in seminal work [Mnih et al., 2015, van Hasselt et al., 2015, Schaul et al., 2015], including frame skips, grayscaling and resizing, reward clipping, no-op starts and terminal-on-life-loss. For DQN and DDQN, we employ the standard network architecture described in Mnih et al. [2015]. SAC employs ReLU activations and the STABLEBASELINES3 standard architecture: two hidden layers of 256 units each.

Table 1: Hyperparameters for SAC on continuous control environments.

PARAMETER	VALUE
LEARNING RATE	$3e - 4$
BUFFER SIZE	$1e6$
BATCH SIZE	256
LEARNING STARTS	$1e4$
DISCOUNT FACTOR	0.99^1
SOFT UPDATE COEFF.	0.005
UPDATE PER STEPS	1
# GRADIENT STEPS	1
OPTIMIZER	ADAM

Table 2: Hyperparameters for DQN on MinAtar.

PARAMETER	VALUE
LEARNING RATE	$2.5e - 4$
BUFFER SIZE	$1e5$
BATCH SIZE	32
LEARNING STARTS	5,000
DISCOUNT FACTOR	0.99
TARGET UPDATE INT.	1,000
STARTING EXPL.	1.0
EXPL. FRACTION	0.05
FINAL EXPL.	0.01
OPTIMIZER	RMSPROP

Table 3: Hyperparameters for DDQN on Atari.

PARAMETER	VALUE
LEARNING RATE	$2.5e - 4$
TOTAL FRAMES	50,000,000
BUFFER SIZE	$1e6$
BATCH SIZE	32
LEARNING STARTS	50,000
DISCOUNT FACTOR	0.99
TARGET UPDATE INT.	30,000
STARTING EXPL.	1.0
EXPL. FRACTION	0.08
FINAL EXPL.	0.01
EVAL EXPL. FRACTION	0.001
TRAIN FREQUENCY	4
GRADIENT STEPS	1
FRAME STACK	4
OPTIMIZER	RMSPROP

Evaluation. For all environments, 100 evaluations were evenly spaced throughout the training procedure. Each agent evaluation consisted of five full trajectories in the environment, going from initial to terminal state. The evaluation score of a single agent evaluation is the average total score across those five evaluation trajectories. SAC employs deterministic action selection during evaluation.

C Implementation details

TA-DDQN The implementation of TA-DDQN is identical to TA-DQN, except that it uses the established DDQN offline target, $\bar{Q}_{target}(S_t) = R_t + \gamma Q(S_{t+1}, \arg \max_{a'} Q(S_{t+1}, a'; \theta); \theta)$ instead of the DQN offline target for alignment calculation and parameter updates.

TA-SAC To adapt the alignment metric for the SAC algorithm, we make specific adjustments to account for both the twin-critic architecture and the maximum entropy objective. For the twin-critic setup, the TD errors and subsequent alignment scores are first computed independently for each of the two Q-networks. To ensure a conservative evaluation of a transition’s utility and prevent overestimation, the final alignment score assigned to each transition is the minimum of the alignment scores across the twin critics. The stochastic policy’s entropy term is integrated into the metric by incorporating it directly into the TD targets. Specifically, the scaled log-probability of the next action, $\alpha \log \pi(a'|s')$, is subtracted from the next-state Q-value estimates for both the online and offline target calculations. This ensures that the alignment calculation evaluates the critics based on the standard soft Bellman equations, requiring no fundamental structural changes to the alignment formulation itself.

D Normalized area under the curve

To evaluate learning efficiency and asymptotic performance simultaneously, we report the nAUC. For a given environment, let R_t denote the mean evaluation return at step t , and let R_{\min} and R_{\max} represent the environment-specific random baseline and the maximum return achieved across all compared algorithms, respectively. To ensure the metric focuses on learning progress relative to the baseline and remains robust to "cold start" noise, we calculate the nAUC by clipping normalized scores at zero and averaging over the total number of evaluation checkpoints T :

$$\text{nAUC} = \frac{1}{T} \sum_{t=1}^T \max \left(0, \frac{R_t - R_{\min}}{R_{\max} - R_{\min}} \right) \quad (12)$$

This metric provides a within-study relative, unitless score in the range $[0, 1]$, where a score of 0 indicates performance no better than a random agent throughout training, and a score of 1 represents achieving the peak performance observed across all conditions at the very first evaluation checkpoint, and maintaining it consistently ever after. We report nAUC across all experimental conditions to provide a statistically sound comparison of sample efficiency.

E Hardware specification

The ATARI experiments were conducted on a workstation equipped with an AMD Ryzen 9 7950X CPU (32 cores at 4.5 GHz), 128 GB of RAM, and an NVIDIA RTX 4090 GPU with 24 GB of memory (CUDA Toolkit version 12.3). All other numerical experiments were performed on a 2024 MacBook Air with an Apple M3 processor.

¹In Swimmer-v4, a discount factor of 0.999 was used.

F Normalized area under the curve tables

Table 4: Normalized Area Under the Curve for Atari-10, standard deviation indicated as \pm .

ENVIRONMENT	DDQN	TA-DDQN	GAIN (%)
AMIDAR	0.325	0.414	+27.4
BATTLEZONE	0.088	0.270	+205.8
BOWLING	0.035	0.193	+446.5
DOUBLEDUNK	0.108	0.296	+175.0
FROSTBITE	0.077	0.338	+337.0
KUNGFUMASTER	0.239	0.298	+24.7
NAMETHISGAME	0.341	0.439	+28.7
PHOENIX	0.113	0.255	+126.5
QBERT	0.201	0.361	+79.3
RIVERRAID	0.216	0.363	+67.9
OVERALL AVERAGE	0.174 \pm 0.10	0.323 \pm 0.07	+151.88 \pm 135.76

Table 5: Normalized Area Under the Curve for continuous control environments, standard deviation indicated as \pm .

ENVIRONMENT	SAC	TA-SAC	GAIN (%)
ANT-V4	0.452	0.534	+18.2
BIPEDALWALKER-V3	0.657	0.784	+19.2
HOPPER-V4	0.630	0.715	+13.5
HUMANOID-V4	0.660	0.733	+11.2
SWIMMER-V4	0.857	0.879	+2.5
WALKER2D-V4	0.587	0.583	-0.7
OVERALL AVERAGE	0.640 \pm 0.12	0.705 \pm 0.12	+10.65 \pm 7.46

Table 6: Normalized Area Under the Curve for experience replay ablations in MinAtar.

CONFIGURATION	ASTERIX	BREAKOUT	FREEWAY	SPACEINVADERS
DQN	0.078	0.256	0.467	0.216
TA-DQN	0.233	0.329	0.610	0.288
DQN + PER	0.049	0.322	0.347	0.161
TA-PER	0.362	0.419	0.648	0.301
DQN + REAPER	0.072	0.263	0.405	0.162
TA-REAPER	0.369	0.336	0.619	0.251

Table 7: Normalized Area Under the Curve for oversampling margin ablations in MinAtar.

CONFIGURATION	ASTERIX	BREAKOUT	FREEWAY	SPACEINVADERS
DQN (BASELINE)	0.086	0.504	0.499	0.275
DQN (2M)	0.105	0.570	0.529	0.342
TA-DQN (B=0.1M)	0.118	0.564	0.565	0.306
TA-DQN (B=0.5M)	0.217	0.580	0.616	0.397
TA-DQN (B=1.0M)	0.254	0.632	0.655	0.353
TA-DQN (B=3.0M)	0.539	0.605	0.728	0.455

G Additional figures

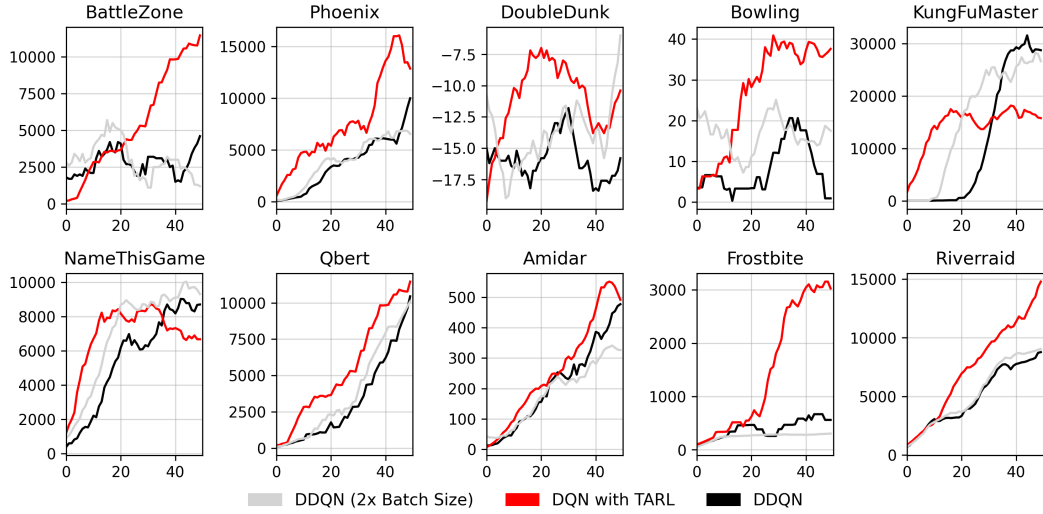


Figure 6: Per-game performance comparison between DDQN and TA-DDQN on the Atari-10 benchmark. Curves represent returns, smoothed over 10 evaluations.

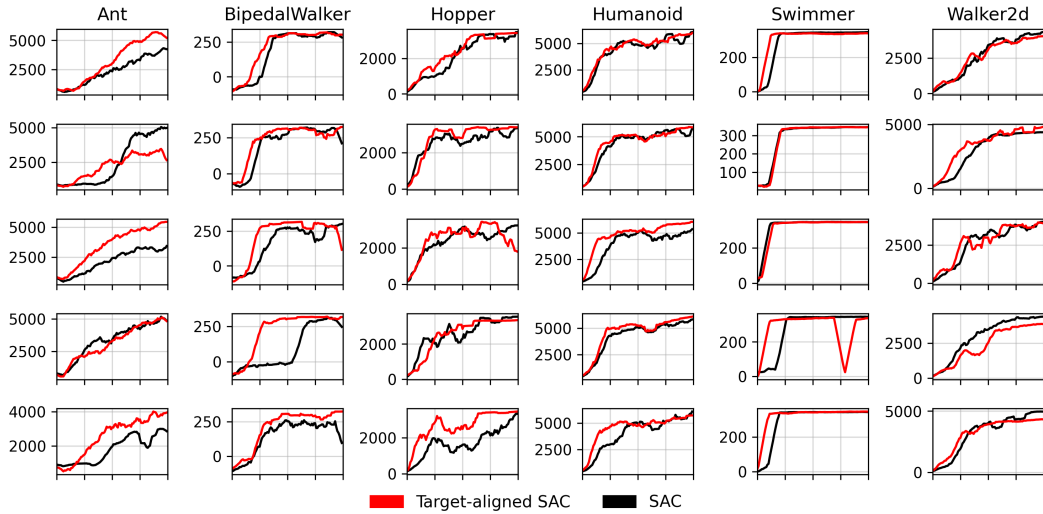


Figure 7: Per-seed performance comparison between SAC and TA-SAC on six continuous control environments. Curves represent returns, smoothed over 10 evaluations.

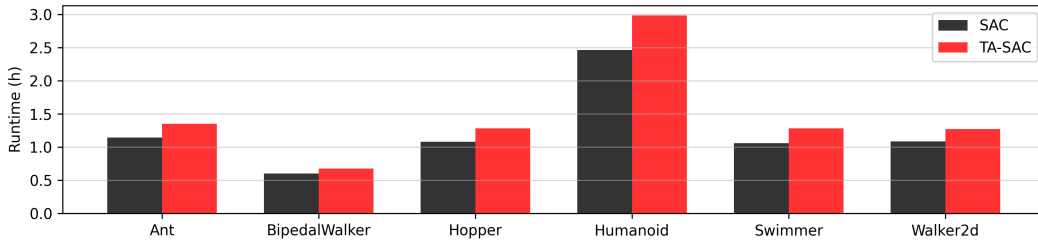


Figure 8: Wall-clock training time for SAC and TA-SAC on six continuous control environments.

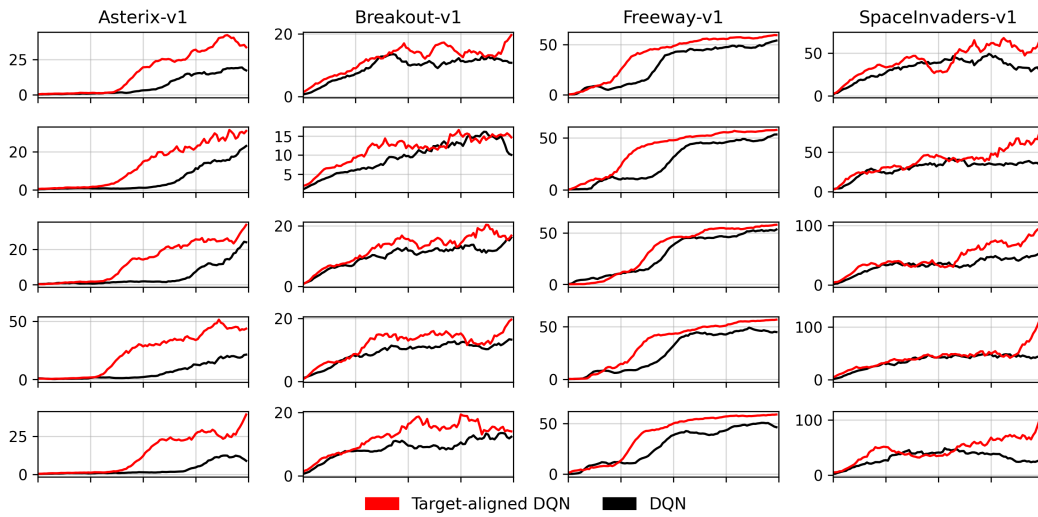


Figure 9: Per-seed performance comparison between DQN and target-aligned TA-DQN on four games of the MINATAR benchmark. Curves represent returns, smoothed over 10 evaluations.

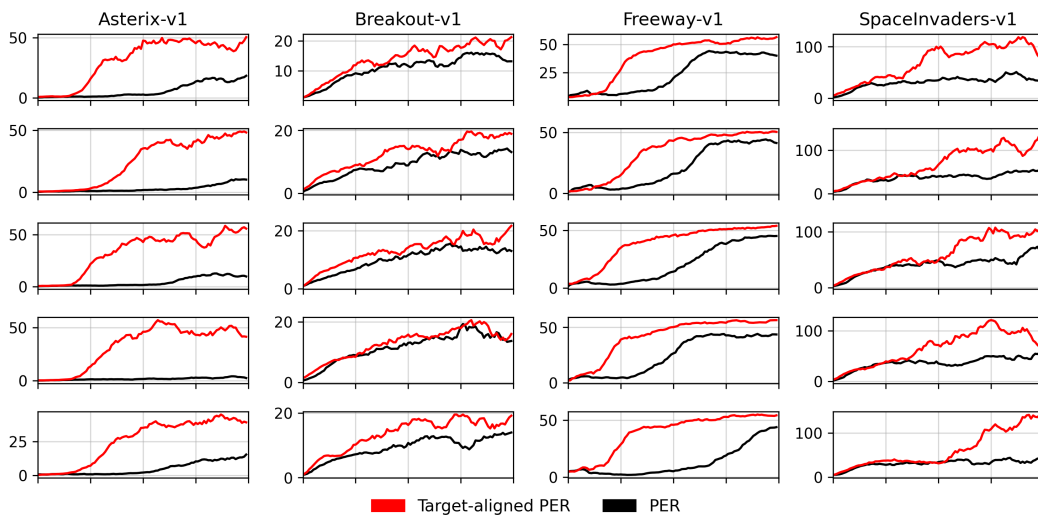


Figure 10: Per-seed performance comparison between DQN with PER and TA-DQN with PER on four games of the MINATAR benchmark. Curves represent returns, smoothed over 10 evaluations.

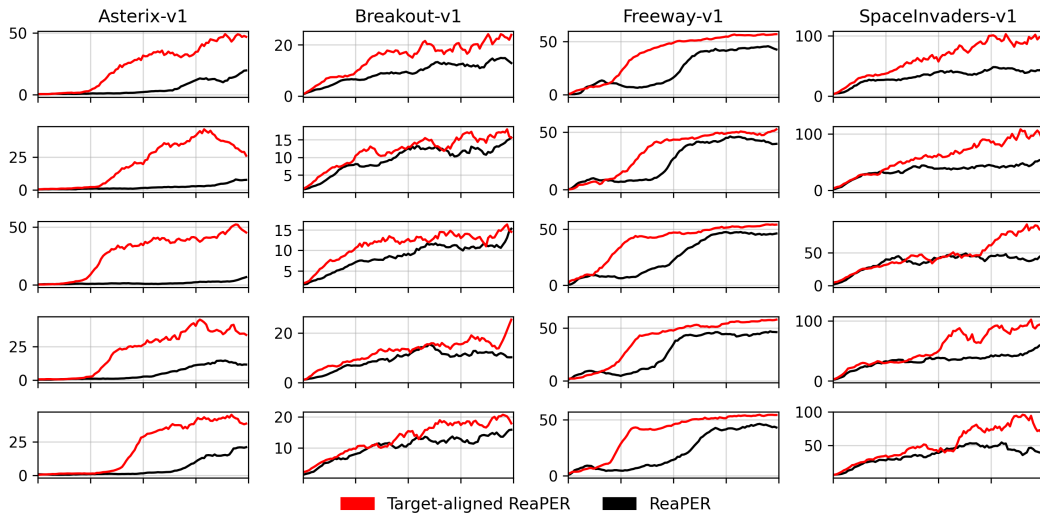


Figure 11: Per-seed performance comparison between DQN with ReaPER and TA-DQN with ReaPER on four games of the MINATAR benchmark. Curves represent returns, smoothed over 10 evaluations.

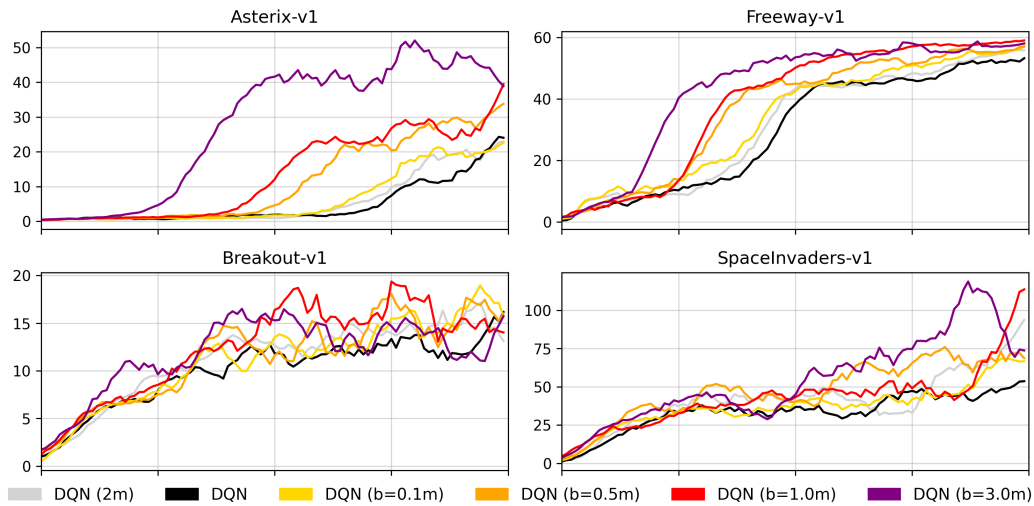


Figure 12: Performance by oversampling margin ($b =$ oversampling margin, $m =$ batch size). Curves represent returns, smoothed over 10 evaluations.

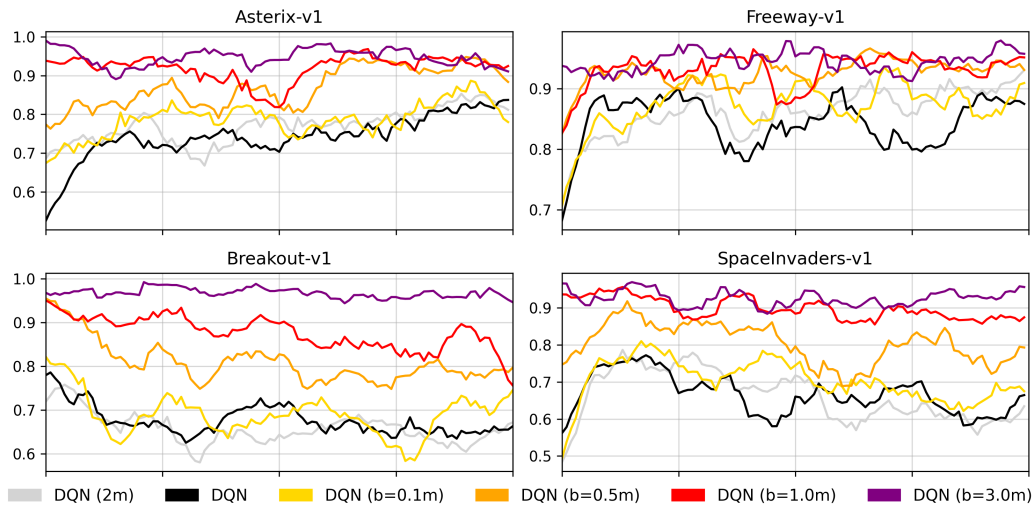


Figure 13: Mean batch alignment by oversampling margin ($b =$ oversampling margin, $m =$ batch size).

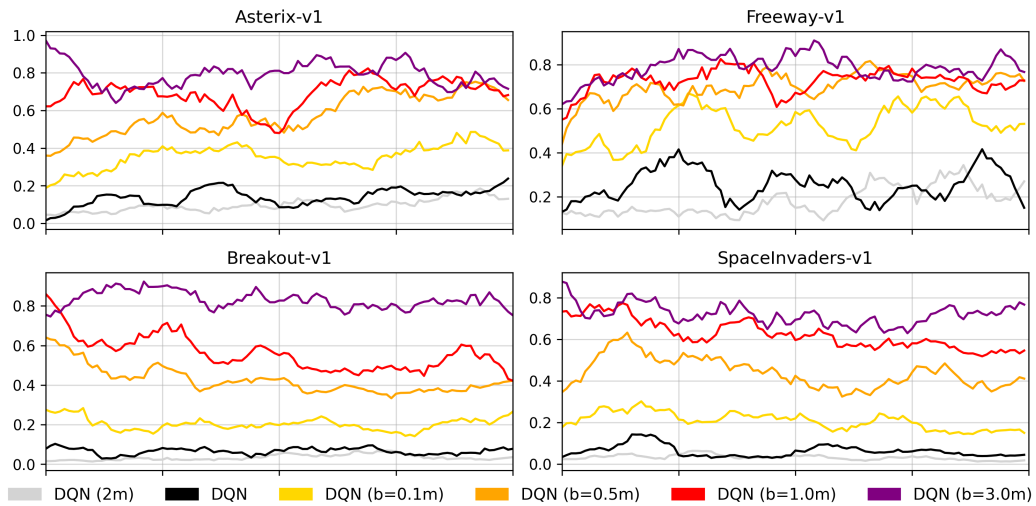


Figure 14: Minimum batch alignment by oversampling margin ($b =$ oversampling margin, $m =$ batch size).